Physica Medica 77 (2020) 138–145

Contents lists available at ScienceDirect

Physica Medica

journal homepage: www.elsevier.com/locate/ejmp

Original paper

Characterization and clinical validation of patient-specific three-dimensional printed tissue-equivalent bolus for radiotherapy of head and neck malignancies involving skin

Brandon A. Dyer[a,*], David D. Campos[b], Daniel D. Hernandez[b,c], Cari L. Wright[b], Julian R. Perks[b], Steven A. Lucero[d], Arnaud F. Bewley[e], Tokihiro Yamamoto[b], Xiandong Zhu[c], Shyam S. Rao[b,*]

[a] University of Washington, Department of Radiation Oncology, Seattle, WA, United States
[b] University of California Davis Comprehensive Cancer Center, Department of Radiation Oncology, Sacramento, CA, United States
[c] University of California Davis, Department of Physics, Davis, CA, United States
[d] University of California Davis, Department of Biomedical Engineering, Electrical & Mechanical Prototyping, Davis, CA, United States
[e] University of California Davis, Department of Otolaryngology Head & Neck Surgery, Sacramento, CA, United States

ARTICLE INFO

Keywords:
Three-dimensional bolus
3D bolus
Bolus
3D printing
Cutaneous malignancies
Photon radiotherapy
IMRT
Dose build-up
Air gaps
Head and neck radiotherapy

ABSTRACT

Purpose: Megavoltage radiotherapy to irregular superficial targets is challenging due to the skin sparing effect. We developed a three-dimensional bolus (3DB) program to assess the clinical impact on dosimetric and patient outcomes.

Materials and Methods: Planar commercial bolus (PCB) and 3DB density, clarity, and net bolus effect were rigorously evaluated prior to clinical implementation. After IRB approval, patients with cutaneous or locally advanced malignancies deemed to require bolus for radiotherapy treatment were treated with custom 3DB.

Results: The mean density of 3DB and PCB was of 1.07 g/cm 3 and 1.12 g/cm3, respectively. 3DB optic clarity was superior versus PCB at any material thickness. Phantom measurements of superficial dose with 3DB and PCB showed excellent bolus effect for both materials. 3DB reduced air gaps compared with PCB - particularly in irregular areas such as the ear, nose, and orbit. A dosimetric comparison of 3DB and PCB plans showed equivalent superficial homogeneity for 3DB and PCB (3DB median HI 1.249, range 1.111–1.300 and PCB median HI 1.165, range 1.094–1.279), but better conformity with 3DB (3DB median CI 0.993, range 0.962–0.993) versus PCB (PCB median CI 0.977, range 0.601–0.991). Patient dose measurements using 3DB confirm the delivered superficial dose was within 1% of the intended prescription (95% CI 97–102%; P = 0.11).

Conclusions: 3DB improves radiotherapy plan conformity, reduces air gap volume in irregular superficial areas which could affect superficial dose delivery, and provides excellent dose coverage to irregular superficial targets.

1. Introduction

Modern linear accelerators delivering megavoltage (MV) energies result in a significant skin sparing effect due to superficial electron disequilibrium in the dose build-up region. The effect of dose build-up in superficial tissues is prominent, and the dose maximum (D_{max}) is not reached until a tissue depth of approximately 1.5 to 1.6 cm with 6 MV photons [1]. The build-up region is problematic when skin coverage is required and is particularly challenging when trying to achieve homogenous dose distributions for irregularly shaped head and neck (H &N) radiation targets (pinna, nose, orbit). In some situations, the use of superficial or orthovoltage photons or electrons may be beneficial. However, for locally advanced disease or complex treatment geometries these techniques may be insufficient.

Traditionally, water-/tissue-density equivalent planar commercial bolus (PCB) or molded wax was positioned over the treatment region to overcome the skin sparing effect. PCB is often a low durometer, semi-transparent synthetic oil gel that comes in uniform sheets of 5–10 mm thickness that are cut and trimmed by hand. For large, flat surfaces PCB provides excellent tissue conformity and dosimetric outcomes [1]. For complex concave/convex superficial radiation targets (nose, pinna, periorbital tissue, jawline, scalp vertex) poor skin-to-bolus conformity

* Corresponding authors at: University of California Davis Comprehensive Cancer Center, Department of Radiation Oncology, 4501 X Street, Suite G-140, Sacramento, CA 95817, United States. University of Washington, Department of Radiation Oncology, 1959 NE Pacific Street, Box 356043, Seattle, WA 98195-6043 (B.A. Dyer).
E-mail addresses: badyer@uw.edu (B.A. Dyer), sdrao@ucdavis.edu (S.S. Rao).

https://doi.org/10.1016/j.ejmp.2020.08.010
Received 24 February 2020; Received in revised form 6 August 2020; Accepted 9 August 2020

can result in air gaps which may negatively impact superficial dose [1–5]. While wax bolus can be used for enhanced surface conformity this material is susceptible to deformation due to temperature, humidity, and storage conditions. Therefore, wax cannot be reliably used for reproducible surface dose enhancement or tissue compensation.

Three-dimensional printed bolus (3DB) precisely matches the patient surface contour. There is burgeoning clinical interest in 3D printing patient-specific custom bolus. Reports on 3DB to date have largely been pre-clinical technical papers with phantom dosimetric evaluations, simple electron plans [1,6,7], or use hard plastics which poorly conform to anatomic changes during radiotherapy (RT) treatment. These hard plastics, such as polylactic acid (PLA), are biodegradable and may potentially degrade under certain storage conditions, thus possibly affecting the bolus effect of both printed materials and raw source materials. The rigid nature of these materials may also yield poor superficial skin-bolus conformality if there is soft tissue swelling and/or tumor growth/shrinkage once treatment begins. Therefore, rigid materials are not ideal as a bolus material – particularly for complex head and neck treatment sites. Alternatively, flexible silicone 3DB has been described [8], but due to the opaque nature of silicone it is difficult to confirm accurate and reproducible clinical placement. Furthermore, published work describing 3D printed bolus with flexible bolus materials, such as thermoplastic polyurethane (TPU), have used simple fixed beam tangent approaches, or with *en face* electrons.

Herein, we present our clinical experience treating H&N patients using a novel, flexible, translucent, patient-specific 3D printed bolus using open source software for broad clinical implementation and end-user flexibility. The specific advancement this work provides is a detailed physical comparison of common planar commercial bolus to 3DB alternatives for patients treated with 3DB and requiring complex H&N photon intensity modulated radiation treatment (IMRT), or with *en face* treatments requiring range modulation, or treatments with integrated shielding. This has not been previously reported in the literature. We characterize the bolus (1) density, (2) dosimetric properties, (3) optic clarity and (4) surface conformality. We also describe our 3DB printing workflow and demonstrate the successful clinical application treating patients using 3DB.

2. Materials/methods

2.1. 3D bolus material and printing

Clear Stratasys TangoPlus 3D bolus material (Stratasys Ltd., Eden Prairie, MN) and an Objet260 Connex3 printer (Stratasys Ltd., Eden Prairie, MN) was used for all 3D printing applications. Print settings and print optimization are automatic based on the printer and material used. The printer is capable of 16 μm layer thickness printing. A water soluble 3DB "raft" printing support structure (Stratasys Ltd., Eden Prairie, MN) is automatically optimized (geometry and orientation) by the printer software to minimize material waste and print time. The "digital materials mode" was set as the default print mode and 100% material in-fill was used. Print speed and total print time vary depending on the 3DB size (volume) and bolus complexity. Typical printing time is 5–18 h and can be performed in parallel with other steps of treatment planning and plan quality assurance, Fig. 1.

2.2. Bolus physical characterization

A pyramid-step 3D structure ranging from 0.2 to 5 cm thickness was printed and used to characterize the 3DB physical properties. Planar bolus (Superflab, Radiation Products Design, Inc., Albertville, MN) ranging from 0.5 to 5 cm thickness was used for benchmark comparison. 3DB and PCB was scanned on a 16-slice brilliance big bore CT (Philips Healthcare, Netherlands) with a 2–3 mm slice thickness, and 512x512 pixel matrix, contoured in Philips Pinnacle^3 version 9.10 treatment planning software (TPS), and the structure file was extracted

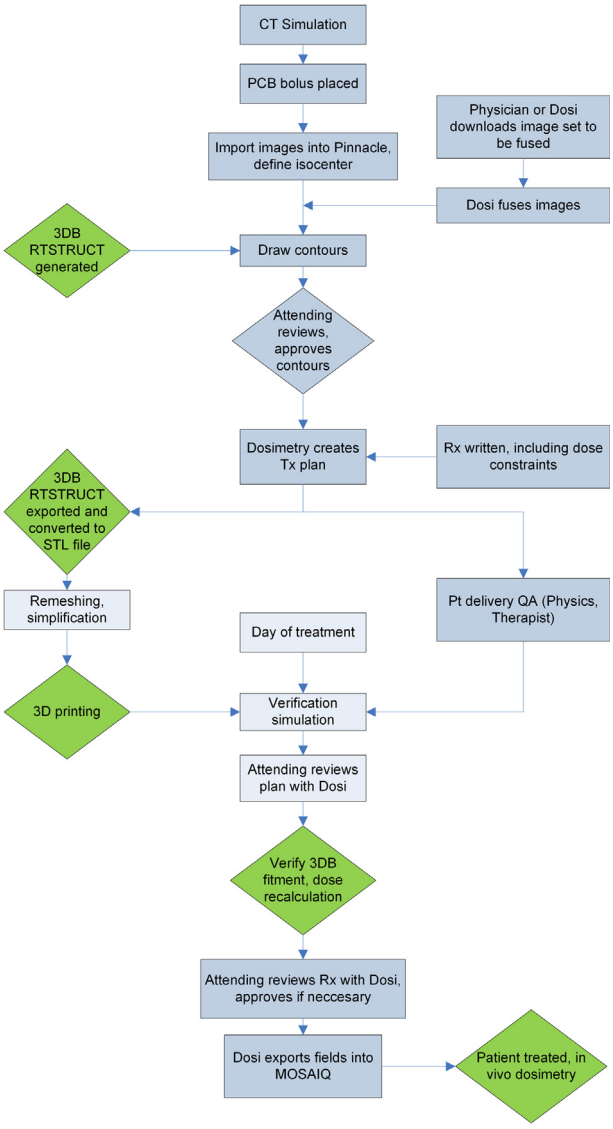

Fig. 1. Clinical workflow for 3DB printing. The workflow is completed using parallel processes, and all process map steps are completed for each 3DB for clinical implementation. Abbreviations: 3DB – three-dimensional bolus, CT – computed tomography, Dosi - dosimetry, PCB – planar commercial bolus, QA – quality assurance, Tx - treatment, Rx - prescription, STL – stereolithography.

using Fiji [9,10]. A 1 mm rind was subtracted from the bolus contour to exclude voxels at the air-bolus interface which introduce uncertainty in CT number measurement due to spatial averaging. CT number was extracted from Pinnacle using the ROI statistics tool. Bolus density was calculated from CT number using a CT-to-density table [11]. Experimentally determined bolus density was compared with published specifications based on 10 independent measurements [12,13].

Bolus optic clarity, defined as the ratio of detectable transmitted-to-incident light deflected by ≤ 2.5 degrees, was determined by illuminating bolus with a 5 mW, 532 nm laser light source (Coherent Inc.) incident on the bolus sample of interest with transmitted light detected via photodiode (Newport 818-BB-40). Entrance and receiving apertures were placed before and after bolus sample, respectively, to limit scattered light from entering the photodiode. The bolus sample was mounted to a 1-D translational stage to obtain clarity measurements at approximately 20 discrete locations (0.5 mm spacing) and averaged for each sample thickness. An optical chopper with a chopping frequency of 500 Hz was placed in the beam path to enable noise suppression of the photodiode signal with Fourier analysis. Fourier analysis was

performed using Labview software to measure the amplitude of the time-averaged (1 s) detected signal from the photodiode at the fundamental frequency of the optical chopper (500 Hz). This minimizes spectral noise from overhead lighting (120 Hz), shot-noise, and Johnson-Nyquist noise, among other, low-amplitude, spectral contributions.

2.3. Bolus dose quality assurance

Quality assurance (QA) testing for PCB and 3DB comparing *in silico* calculations and *in vitro* measurements was performed using an anthropomorphic phantom. Small volume (IMRT) metal oxide semiconductor field effect transistor (MOSFET) were affixed to the phantom with paper tape and calibration was performed by delivering 200 cGy dose (n = 10) on a clinical Elekta-Synergy linear accelerator. MOSFETs were placed in the center of the irradiated field, or in the high-risk clinical target area. Planar commercial bolus (PCB) or 3DB were then placed on the phantom on top of the MOSFETs to determine the net bolus effect in the irradiated area. Superficial dose was then measured under a variety of clinical scenarios. All calibration and bolus measurements were performed using a 10x10 cm field and 6 MV beam at 100 cm source-skin distance (SSD) with a 1 cGy/monitor unit (MU) calibration factor.

2.4. 3DB clinical implementation and study participants

After institutional review board (IRB) approval, H&N patients were enrolled, treated, and a retrospective analysis of the 3DB intervention for patients treated between 9/2016 and 10/2017 was performed. All H&N patients were eligible if bolus was clinically indicated. No exclusion was made based on disease subsite, tumor histology, tumor stage, patient age, sex, or performance status. A cohort of 10 case-matched patients was used to evaluate air gap differences at the time of simulation and during treatment. Patients were treated with either volumetric modulated arc therapy (VMAT) or *en face* electrons.

2.5. Computed tomography (CT) simulation

Prior to computed tomography (CT) simulation (SIM), PCB was cut and positioned over the radiotherapy (RT) treatment site and fastened using a variety of methods to minimize air gaps. All simulations were completed on a 16-slice brilliance big bore CT (Philips Healthcare, Netherlands) with a 2–3 mm slice thickness, and 512x512 pixel matrix covering an appropriate anatomic region. CT images were processed using Philips software and sent to Philips Pinnacle^3 version 9.10 TPS for organ and target segmentation, and RT treatment planning. A clinical workflow for 3DB fabrication is shown in Fig. 1. CT density was determined using our institutional Pinnacle density table using eight different materials to cover the full range of densities expected in clinical treatment ranging from air to metallic implants. The density properties (both physical and electron) are so close to water that differences due to material properties are minute.

2.6. Generation and evaluation of 3DB

The 3DB structure was generated in Pinnacle TPS (3DB-RTSTRUCT) by drawing the desired 3DB structure. Variable bolus thickness is possible depending on the goals of treatment (tissue compensation, organ at risk (OAR) sparing, *etc*), Fig. 2A. A density was assigned to the 3DB structure in the TPS for dose calculations (1 g/cm^3). Assigning the 3DB-RTSTRUCT a density is necessary as, without a density correction, the treatment planning system would not recognize the 3DB as a structure with physical density, and dose calculations would be inaccurate. 1 g/cm3 was used to represent the physical density of water, which approximates the density of the bolus material as measured experimentally within one significant digit. The 3DB-RTSTRUCT was exported from the TPS and converted to a stereolithography (STL) file using open-source Slic3r G-code generator 4.5.0 (http://slic3r.org/) which is compatible with open-source Meshmixer 3D printer software (http://meshmixer.com/) for remeshing, mesh simplification and structure smoothing prior to printing, Fig. 2B-C. Detailed instructions for file conversion and remeshing are available in the Appendix.

In silico dose calculation was performed within the Pinnacle TPS. Pinnacle uses an adaptive convolution superposition algorithm for all dose calculations regardless of medium. The algorithm consists of four components: modeling incident fluence from the linear accelerator head, projection of the fluence through the density representation of the patient media to determine TERMA (total energy released per unit mass), three dimensional superposition of the TERMA with the energy deposition kernels, using a ray-tracing technique, to incorporate the effects of heterogeneities on lateral scatter, and finally modeling of electron contamination by exponential falloff. The grid size chosen for the 3DB calculation was the departmental standard 2.5 mm sided voxel. In the absence of full photon Monte Carlo algorithm the adaptive convolution superposition is widely regarded as the industry standard and as such is expected to produce clinically acceptable results in the case of dose distributions under the 3DB.

The effect of 3DB and PCB on dose build-up were evaluated using an anthromorphic phantom and superficial dose delivery of 200 cGy was quantified using MOSFET measurements (n = 10). Measurements were taken from flat and curved phantom surfaces, both with and without bolus. PCB placement on curved phantom surfaces induces shear stress in the bolus due to the pliable nature of the material; this effect was not seen with 3DB.

After verification that 3DB had similar physical and dose buildup properties as PCB we evaluated the clinical use. Patients undergoing treatment for locally advanced H&N cancer involving the skin underwent standard simulation with PCB. Then, during treatment planning, the 3DB-RTSTRUCT was generated and printed. After 3DB printing, but prior to initiation of treatment, patients received a verification CT simulation or cone beam CT immediately prior to treatment to confirm conformal bolus fitment, and for secondary dose calculation, Fig. 2. Air gap volume, defined as the volume between the inner bolus and skin surface, was contoured for both PCB and 3DB and determined at $>$ 5 mm from the skin surface. The 5 mm distance was used as a threshold which has been previously shown to negatively impact superficial dose [3,14]. Dose to superficial RT targets ($\leq$5 mm deep to skin surface) was compared for PCB or 3DB using homogeneity index (HI) and conformity index (CI) with respect to tissue, more specifically, the high-risk clinical target area – the location of tumor in the superficial skin – using standard definitions [14]. Finally, for clinical validation, the intended prescription dose was compared with *in vivo* small volume MOSFET measurements for patients receiving radiation therapy with 3DB.

Calculated point dose from multiple areas beneath the 3DB were validated against physical MOSFET measurements. This approach is an adequate representation of superficial dose as all patients treated have skin involvement and multiple MOSFET measurements are obtained from beneath the bolus in the area of the tumor, thus capable of detecting adequate dose coverage of the radiation target. At the time of MOSFET measurement detailed clinical photographs of MOSFET placement were taken, and the treating attending physician was physically present to place the detectors. The same physician, in consultation with the medical physicist, derived the expected dose from the TPS. This method produces dose calculation points accurate to the measurement point within 2 mm, which matches the TPS dose calculation grid even where intensity modulation has been used.

2.7. Statistical methods

Descriptive statistical comparison of 3DB and PCB was performed using unpaired, one-tailed *t*-test with significance set at $p < 0.05$. Bolus optic clarity was compared using a multivariate exponential

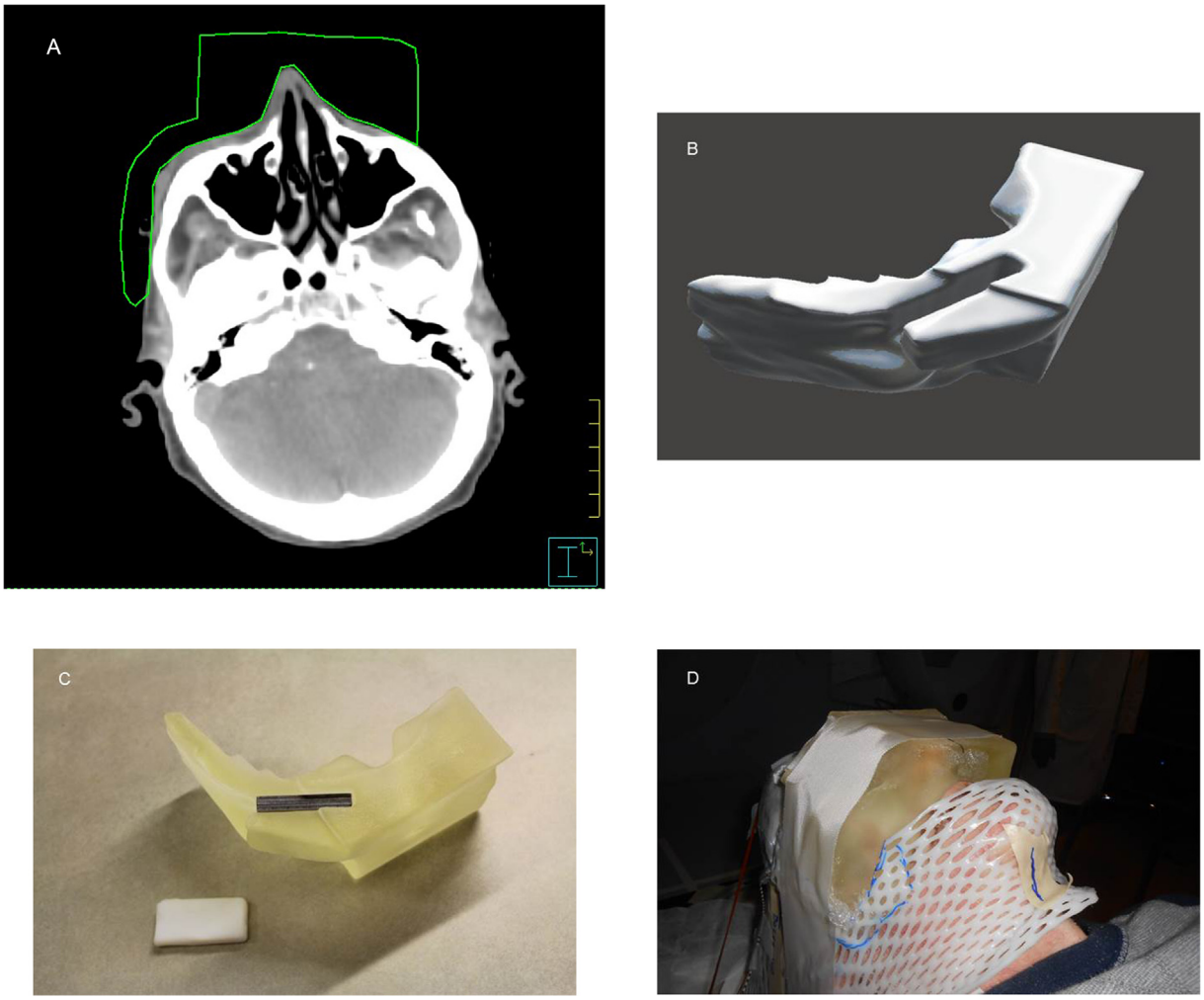

Fig. 2. 3D bolus RTSTRUCT (A) is converted to an STL file, then remeshed and smoothed (B) prior to final printing (C), and patient use (D). The slot in the bolus material (B) was generated during the remeshing process to accept an integrated stainless steel eye shield (C) to reduce dose to the eye during radiotherapy treatment delivery with electrons. This bolus also incorporates a tissue compensator over the nose. The patient was re-simulated (D) prior to treatment to for verification of bolus conformity and to calculate dose prior to treatment. Abbreviations: STL – stereolithography.

regression model which was necessary to account for bolus material attenuation, material thickness, and surface effects on optic clarity. One-way ANOVA was used to compare the effect of bolus type on air gap size for 3DB and planar bolus. Post hoc comparisons using Tukey HSD testing with Bonferroni correction for multiple comparisons was performed for significant results. All tests were performed in Excel 2010 with Analysis ToolPak.

3. Results

As bolus density directly influences dose in the build-up region, we characterized the physical properties of the bolus materials. The manufacturer published density for the 3DB material [13] was 1.12–1.13 g/cm^3, and 1.03 g/cm^3 for PCB [12]. The measured mean density was significantly different for 3DB versus PCB, 1.07 ± 0.019 g/cm^3 and 1.12 ± 0.018 g/cm^3 , respectively, $p < 0.001$. There was less intra-bolus density variability with 3DB versus PCB, 1.09 g/cm^3 [range 1.07–1.10 g/cm^3] and 1.13 g/cm^3 [range 1.08–1.15 g/cm^3], respectively.

We then evaluated dose build-up using an anthromorphic phantom. The mean output during MOSFET calibration (n = 10) was 198 ± 2.5 cGy. The calculated superficial dose (200 cGy) was compared with phantom MOSFET measurements (n = 10) for dose delivered without bolus, with 3DB, or with PCB with or without bolus traction. Without bolus, the mean phantom dose was 72 ± 4.1 cGy (36% of prescription). Using 1 cm 3DB, the mean dose was 196 ± 3.1 cGy (98% of prescription). Using 1 cm PCB, the mean dose was 195 ± 4.2 cGy (98% of prescription).

Placement of 1 cm PCB on a curved phantom surfaces induces shear stress, and when PCB MOSFET measurements were repeated the mean dose was 193 ± 3.4 cGy (96% of prescription). As 1 cm 3DB did not demonstrate change in shape with shear stress, measurements were not taken. There was a significant difference in measured superficial dose as measured by MOSFET comparing 3DB (196 cGy, 95% CI 194–198 cGy; $p = 0.005$) or PCB (195 cGy, 95% CI 193–198 cGy; $p = 0.01$) versus PCB under shear tension (193 cGy, 95% CI 191–195 cGy).

Clinical bolus placement is achieved by placing the bolus on the patient when aligned to treatment isocenter using a fixed, three-point external laser reference system. Reproducible bolus placement ensures the intended dose is delivered. For 3DB, laser alignment marks can be directly printed into the material during the printing process, Fig. 3. Isodose markings can be created within the 3DB by adding an RTSTRUCT substructure within the bolus structure, or added after export from the TPS in Meshmixer, prior to 3DB printing. The 3D localization contour is transmitted via DICOM to STL, and then interpreted in the CAD software. By setting the localization mark to be printed with black material the 3DB isocenter mark can be printed in. One drawback with this approach is that a material change during 3D printing is necessary.

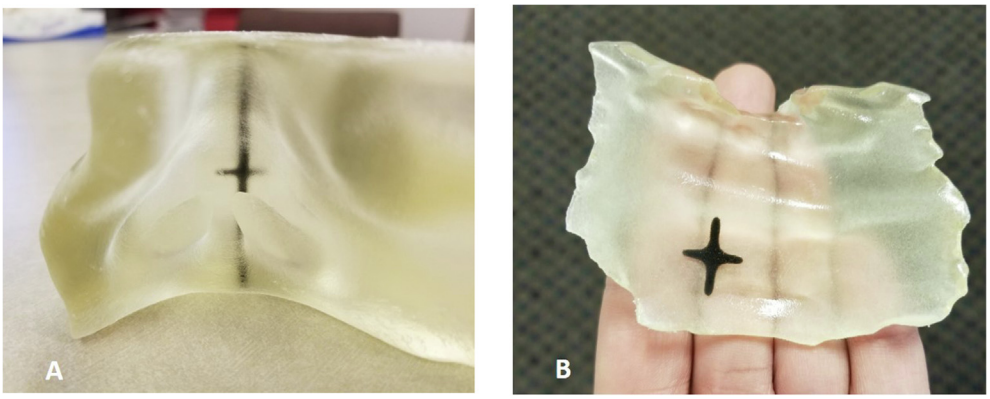

Fig. 3. Examples of 3D bolus used to treat a skin malignancy involving the nose (A) and lip (B) are shown. The black cross provides built-in daily setup localization at the treatment isocenter for use with an in-room laser alignment system. This mark has been printed into the bolus and aids in rapid, reproducible bolus placement. Panel B demonstrates the excellent bolus clarity.

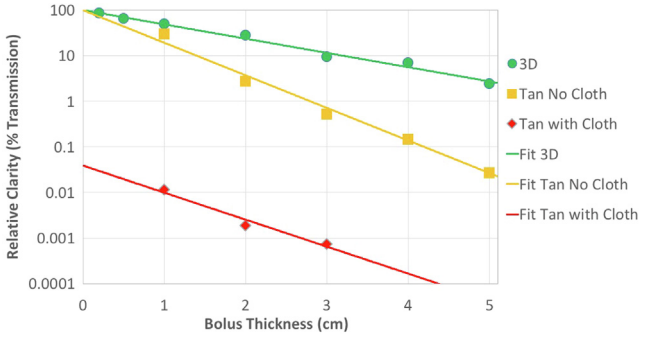

Fig. 4. Quantitative bolus optic clarity is shown for 3D bolus (3DB), and for planar commercial bolus (PCB) with and without cloth backing. 3DB optic clarity is superior to PCB at any bolus thickness.

For PCB, due to the oil-based material properties, it is difficult to directly mark the material and a cloth-backed version is frequently employed which prevents direct visual confirmation of bolus placement. Bolus optic clarity measurements are shown in Fig. 4. At 0.5 cm bolus thickness, clarity was 70% for 3DB versus 44% with new, clinically unused PCB (no cloth backing) versus 0.02% with new, clinically unused PCB (with cloth backing). Bolus clarity at 1 cm thickness was 39% for 3DB and 19% for new, clinically unused PCB without cloth backing. After > 1 cm bolus thickness, clarity decreases considerably for all materials.

Bolus surface conformity was determined by the air gap volume (cubic cm, cc) and distance between the inner surface of the bolus and skin surface, Fig. 5. The total air gap volume beyond the skin surface was less with 3DB (median 7 cc, range 5–39) compared with PCB (median 17 cc, range 13–68). Additionally, PCB had greater air gap volume > 5 mm from the skin surface in the high-risk planning target

Table 1
Comparison of air gaps at the time of computed tomography (CT) simulation (SIM), and from daily treatment verification cone beam computed tomography (CBCT) imaging at the beginning (CBCT1), middle (CBCT2), and end (CBCT3) of treatment. One-way ANOVA analysis comparing air gaps for patients treated with 3DB and planar bolus demonstrate a significant reduction with 3DB relative to planar bolus. Post hoc comparison using the Tukey HSD with Bonferroni correction for multiple comparisons indicated that the mean air gap volume for 3DB was significantly different from planar bolus for all metrics ($P < 0.05$). Taken together, these results suggest that 3DB has a significant effect on air gaps – notably in high-risk irregular areas and may provide superior dose to superficial radiation targets compared with planar bolus. Abbreviations: 3DB – three-dimensional bolus, cc – cubic centimeters.

Patient	Disease site	Bolus Type	Image source	Total air gap volume, cc	Air gaps beyond 5 mm of skin surface, cc
1	Skin, orbit/ nose	3DB	CT SIM	1.32	0
			CBCT1	0.17	0
			CBCT2	0.78	0
			CBCT3	0.45	0
2	Skin, pinna/ scalp	3DB	CT SIM	3.41	0
			CBCT1	1.67	0.02
			CBCT2	5.65	0.26
			CBCT3	5.72	0.01
3	Skin, pinna	3DB	CT SIM	1.04	0
			CBCT1	0.13	0
			CBCT2	1.14	0
			CBCT3	4.72	0
4	Skin, nose	Planar	CT SIM	19.03	1.69
5	Skin, scalp	Planar	CT SIM	28.82	0.75
6	Skin, pinna	Planar	CT SIM	20.62	0.93
			CBCT1	45.68	1.42
			CBCT2	27.58	1.11
			CBCT3	59.23	3.41

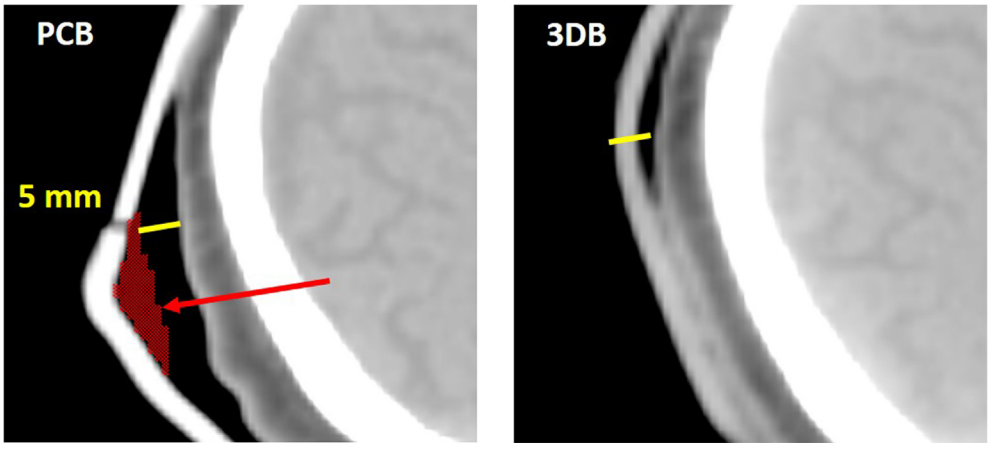

Fig. 5. Representative air gap differences for planar bolus (*left*) and 3DB (*right*) are shown. The yellow bar is 5 mm. The area in red color wash (*left*) shows an air gap beyond 5 mm from an irregular skin radiation target surface. Air gaps beyond 5 mm of the skin surface have been shown to negatively impact radiation delivery at the skin surface. The total air volume beneath the bolus was less with 3DB (median 7 cc, range 5–39) compared with PCB (median 17 cc, range 13–68). Additionally, PCB had greater air gap volume > 5 mm from the skin surface in the high-risk radiation planning target volume region (median 0.81 cc, range 0.80–2.5) compared with 3DB (median 0.059 cc, range 0.00–0.078; $P = 0.063$).

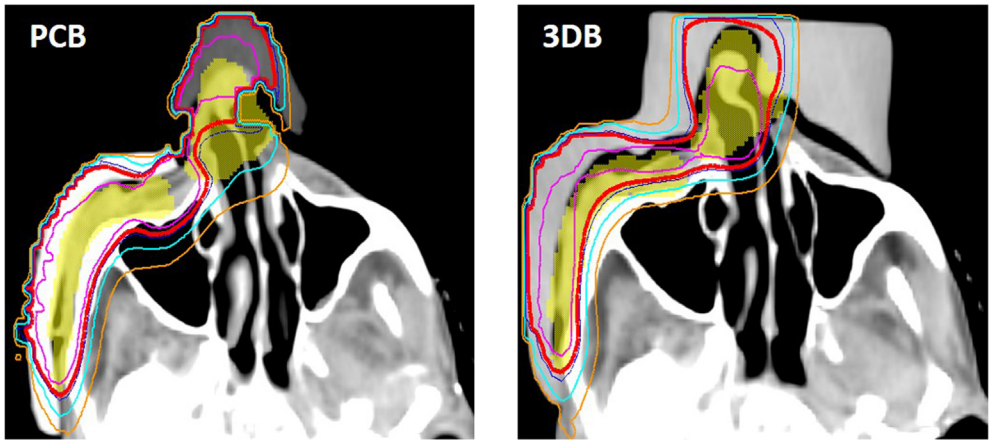

Fig. 6. Representative images comparing homogeneity and conformity for PCB (left) and 3DB (right) for the bolus described in Fig. 2 are shown. The area in yellow color wash is the high-risk radiation planning target volume. The thick red line represents the prescription isodose line (95% of the prescription dose). For this plan, both PCB and 3DB had a heterogeneity index of 1.3. However, the conformity index with 3DB was 0.96, and for PCB was 0.60. Therefore, this indicates that a significant portion of the target volume was not being adequately covered using PCB by the intended prescription. Underdosing the target volume has implications on tumor control.

volume region (median 0.81 cc, range 0.80–2.5) compared with 3DB (median 0.059 cc, range 0.00–0.078; $p = 0.063$). When air gaps were assessed for case-matched patients, one-way ANOVA demonstrated a significant effect on air beneath the bolus, Table 1. The choice of bolus material had a significant effect ($p < 0.05$) on total air volume above the radiation treatment site [$F(2, 23) = 40.0$, $p < 0.01$], and air gap volume $>$ 5 mm beyond the skin surface [$F(2, 23) = 26.1$, $p < 0.01$]. Post hoc comparison indicated the mean total air gap volume was significantly different for 3DB (2.18 ± 2.11 cc) than for planar bolus (33.49 ± 15.76 cc), and for air $>$ 5 mm from the skin surface for 3DB (0.02 ± 0.07 cc) than for planar bolus (1.55 ± 0.97 cc).

A dosimetric comparison of 3DB and PCB plans for the first three patients treated with 3DB was performed to evaluate plan dose homogeneity (HI) and dose conformity (CI), Fig. 6. In these patients, 3DB and PCB had nearly equivalent median dose homogeneity (3DB median HI 1.249, range 1.111–1.300 and PCB median HI 1.165, range 1.094–1.279). However, dose conformity was better with 3DB (median 3DB CI 0.993, range 0.962–0.993 and median PCB CI 0.977, range 0.601–0.991).

After we demonstrated that 3DB can provide accurate superficial dose and, at minimum, dosimetrically-equivalent radiotherapy plans we proceeded with patient treatment, Table 2. MOSFET measurements demonstrated the mean delivered dose as a percentage of the intended dose was within 99% of prescription (95% CI 97–102%; $p = 0.11$) over 104 measurements. Furthermore, all patients treated with 3DB successfully completed radiation as intended with no unexpected toxicity or adverse events during or after treatment.

Finally, our clinical 3DB workflow (Fig. 1) did not cause disruption or delay in initiating patient treatment. After the initial CT simulation, generation of RT target volumes and delineation of OARs takes ≤ 2 days, RT plan generation takes ≤ 3 days, printing of 3DB takes ≤ 3 days of total processing time (file conversion, remeshing, printing), and patient delivery quality assurance (physics and therapist) takes ≤ 1 day.

4. Discussion

The primary clinical utility of bolus is to overcome the "skin-sparing effect" caused by electronic disequilibrium in superficial tissues. Hand-cut planar bolus has long been used to improve superficial RT dose delivery, but this material is often suboptimal for complex H&N geometries due to poor conformity resulting in air gaps that negatively impact superficial dosimetric outcomes. Wax could potentially be used; however, is subject to deformation and degradation and therefore inappropriate to use for reliable superficial dose delivery in critical H&N locations or tissue compensation/range modulation with complex H&N geometries.

Herein, we rigorously and methodically characterized the physical and dosimetric properties of 3DB using a readily-available tissue-equivalent, translucent material. We then clinically implemented a patient-specific conformal 3DB printing program to improve superficial dose to complex H&N radiation targets and demonstrated accurate dose delivery. The techniques and methods presented are applicable to any other treatment site that requires bolus using either photon or electron techniques.

Because H&N radiotherapy requires highly conformal treatment to minimize toxicity to OARs, and the irregular surface topography is dosimetrically challenging, it is an ideal site to validate 3DB for improved clinical treatment solutions. Prior studies evaluated 3DB use in the H&N; however, these studies were pre-clinical, focused on technical

Table 2
Metal oxide semiconductor field effect transistor (MOSFET) measurements of dose delivered to the first 10 patients treated with 3DB. Mean dose is shown as a percent of the intended prescription dose, including standard deviation. Taken together, the delivered dose was 99% of the intended prescription dose (95% CI 97–102%; $P = 0.11$) over 104 measurements. No patient treated with 3DB developed unexpected treatment-related toxicity or discontinued treatment. Abbreviations: AJCC 8 – American Joint Committee on Cancer 8th Edition, CTCAE – Common Terminology Criteria for Adverse Events Version 4.0, H&N – head and neck.

Patient	Age	H&N Site	AJCC 8 Stage	MOSFET Readings, #	Mean Dose Relative to Prescription, %	Worst Toxicity, CTCAE v 4.0	Unexpected Toxicity	Discontinued Treatment
1	51	Larynx	IVA	11	105 ± 4%	G3 skin erythema	None	No
2	55	Skin, face	II	4	103 ± 3%	G2 skin erythema	None	No
3	78	Skin, scalp	II	19	99 ± 4%	G2 skin erythema	None	No
4	67	Skin, face	III	8	97 ± 5%	G2 skin erythema	None	No
5	75	Skin, eye	I	9	102 ± 5%	G2 skin erythema	None	No
6	54	Skin, ear	I	16	97 ± 3%	G1 skin erythema	None	No
7	93	Skin, ear	IV	13	97 ± 13%	G2 skin erythema	None	No
8	84	Skin, scalp	IV	8	98 ± 3%	G1 skin erythema	None	No
9	87	Skin, face	IV	6	98 ± 4%	G1 skin erythema	None	No
10	86	Skin, face	IV	10	98 ± 5%	G1 skin erythema	None	No

development and dosimetric comparison, or were used in sites with minimal surface contour change (i.e., breast) [15–17]. Early reports on 3D printing for radiotherapy bolus used computer aided design (CAD) software and computer numerical control (CNC) milling with non-pliable, opaque materials [18]. However, clinical recognition that opaque and rigid materials are difficult to place clinically, and poorly conformal to complex surface anatomy changes during RT led to the pursuit of alternative methods and materials [8].

Phantom measurement of commercial and 3D printed bolus density showed that both materials are close to water-/tissue-density (1.0 g/cm^3). However, 3DB density is more uniform, and not susceptible to distension which can alter dose attenuation and buildup. Furthermore, our 3DB is flexible and maintains excellent surface conformity for accurate positioning. This is important in the clinically-relevant photon beam energy range (6–10 MV) where Compton scatter is predominant and is roughly proportional to mass density for most materials [19]. We found that when PCB is subject to shear or tensile stress and deforms it affects delivered superficial dose in a small (but significant) way, impacting both superficial dose and/or homogeneity, thus plan quality.

With respect to accuracy of clinical set-up, analysis of bolus optic clarity showed 3DB was vastly superior to PCB. Improved 3DB optic clarity aids accurate daily treatment placement and provides direct visual confirmation that the bolus is correctly positioned. Furthermore, accuracy of clinical placement has implications on superficial dose [3].

Using 3DB, we found a reduction in total air gap volume between the skin and inner bolus surface and, more importantly, in air gap volume in irregular (pinna, nose, orbit) high-risk radiation target areas. This finding has distinct dosimetric implications on superficial dose, and possibly on tumor control [3]. Both Khan et al and Sroka et al evaluated the effect of air gaps at the tissue-bolus interface during RT and found that surface dose was affected by increasing air gaps – particularly in the dose buildup region [1,5]. Fujimoto et al evaluated the feasibility of using rigid acrylonitrile butadiene styrene (ABS) material for 3DB photon RT and found that 0.5 cm 3DB and PCB resulted in equivalent *in silico* Dmax (0.6 cm); however, phantom measurements showed that 3DB was closer to calculated doses than PCB, and more conformal [4]. Given the variability of day-to-day patient treatment setup, the larger air gap volume seen with PCB could lead to underdosing the radiation target in the high-risk region which may result in inferior local tumor control.

While radiotherapy plan dose homogeneity is comparable for 3DB and PCB, dose conformity is better with 3DB – particularly for irregular radiation targets. The predominant reason that 3DB produces more conformal superficial radiation dose compared with PCB is that complex concave/convex geometries (particularly with changing curve radius) can be engineered seamlessly with 3DB. With planar bolus, changes in surface curvature require cutting and/or plication of the bolus material to improve surface conformity. However, by nature, cutting or folding a planar bolus material will introduce irregularities and/or air gaps. The magnitude and extent of these gaps depends on the size of the area requiring coverage, and the spacing/depth of the irregular contour. Furthermore, the ability to manipulate 3DB thickness during the treatment planning stage provides additional treatment delivery degrees of freedom and treatment flexibility (Fig. 2). Patient MOSFET measurements confirm phantom and dosimetric calculations, with excellent net bolus effect.

3DB also has the added advantage of clinical ease of use. The translucent 3DB material facilitates direct visual confirmation of clinical bolus placement and the ability to confirm good conformity between the bolus and skin surface. Anecdotally, we found that the ability to build-in treatment setup marks provides our radiotherapists reassurance of correct bolus placement and decreased patient setup times – particularly for complex treatments involving the nose, pinna, periorbital tissue, jawline, or scalp vertex. Our clinical validation was performed using a complete printing system from a single vendor, inclusive of the printer, automated printer settings, and printing material. Other vendors may have similar material products capable of 3DB production, and result in similar bolus outcomes; however, care should be exercised in using these products clinically without prior validation.

Despite the demonstrable benefits of 3DB for complex geometries, the primary consideration in implementing such a program clinically is selection of a 3D printing platform (manufacturer) and material, as most manufacturers use of proprietary, printer-specific materials. Based on our results we favor a translucent, tissue-equivalent material which facilitates reproducible clinical placement, provides excellent superficial dose, and is highly conformal. In terms of bolus generation, there is a learning curve for the physician in drawing the 3DB structure during the planning stages, for medical dosimetry in learning how to manipulate/alter the bolus structure to achieve the desired superficial dose, and in remeshing and printing the 3DB (see Appendix). The generation and printing of the 3DB can be billed to insurance as part of the CT simulation charge panel consisting of items necessary for immobilization, planning, or treatment.

5. Conclusions

3DB provides an individualized bolus solution to unique and/or irregular patient anatomy. 3DB has a potential advantage over PCB, or other proposed rigid or opaque 3D printed boluses, in several key areas: patient-specific conformality, flexibility, and optic clarity. Accurate bolus placement is enhanced by superior 3DB optic clarity over PCB and the ability to build-in treatment setup marks. Our results show improved radiotherapy plan dose conformity with 3DB. Most importantly, these results serve as one of the first detailed characterizations of patient specific 3D printed bolus with *in vivo* measurements on treated patients confirming accurate dose delivery. Based on our continued 3DB experience, our department routinely uses 3DB for the treatment of malignancies involving skin with irregular or complex surfaces.

6. Funding details

There are no funding sources to disclose. The listed authors declare no actual or potential conflicts of interest. There were no grants, monies or other financial incentives or coercions used or offered in the preparation of this manuscript. This manuscript has not been presented or published, in part or in full, prior to this submission.

7. Ethics board approval

Prior to clinical implementation this study was reviewed by the University of California Davis IRB and was approved under IRB identification number 960240-1.

Declaration of Competing Interest

The authors declare that they have no known competing financial interests or personal relationships that could have appeared to influence the work reported in this paper.

Appendix A. Supplementary data

Supplementary data to this article can be found online at https://doi.org/10.1016/j.ejmp.2020.08.010.

References

[1] Khan Y, Villarreal-Barajas JE, Udowicz M, Sinha R, Muhammad W, Abbasi AN, et al. Clinical and dosimetric implications of air gaps between bolus and skin surface during radiation therapy. Journal of Cancer Therapy. 2013;4:1251.
[2] Robar JL, Moran K, Allan J, Clancey J, Joseph T, Chytyk-Praznik K, et al. Intrapatient study comparing 3D printed bolus versus standard vinyl gel sheet bolus for postmastectomy chest wall radiation therapy. Pract. Radiat Oncol. 2017.
[3] Butson MJ, Cheung T, Yu P, Metcalfe P. Effects on skin dose from unwanted air gaps

under bolus in photon beam radiotherapy. Radiat Meas 2000;32:201–4.
[4] Fujimoto K, Shiinoki T, Yuasa Y, Hanazawa H, Shibuya K. Efficacy of patient-specific bolus created using three-dimensional printing technique in photon radiotherapy. Phys Med. 2017;38:1–9.
[5] Sroka M, Regula J, Lobodziec W. The influence of the bolus-surface distance on the dose distribution in the build-up region. Rep Pract Oncol Radiother. 2010;15:161–4.
[6] Perkins GH, McNeese MD, Antolak JA, Buchholz TA, Strom EA, Hogstrom KR. A custom three-dimensional electron bolus technique for optimization of post-mastectomy irradiation. Int J Radiat Oncol Biol Phys. 2001;51:1142–51.
[7] Canters RA, Lips IM, Wendling M, Kusters M, van Zeeland M, Gerritsen RM, et al. Clinical implementation of 3D printing in the construction of patient specific bolus for electron beam radiotherapy for non-melanoma skin cancer. Radiother Oncol. 2016;121:148–53.
[8] Chiu T, Tan J, Brenner M, Gu X, Yang M, Westover K, et al. Three-dimensional printer-aided casting of soft, custom silicone boluses (SCSBs) for head and neck radiation therapy. Pract. Radiat Oncol. 2017.
[9] Schindelin J, Arganda-Carreras I, Frise E, Kaynig V, Longair M, Pietzsch T, et al. Fiji: an open-source platform for biological-image analysis. Nat Methods. 2012;9:676–82.
[10] Schindelin J, Rueden CT, Hiner MC, Eliceiri KW. The ImageJ ecosystem: An open platform for biomedical image analysis. Mol Reprod Dev. 2015;82:518–29.
[11] Ly-Ba A, Abdallah OA, Ba-Diop S, Ly-N'Diaye Fbadiane M, Sarr M, et al. Mali Med 2007;22:54–7.
[12] Pouye A, Ndong S, Diallo S, Ba Diop S, Fall S, Leye A, et al. Senegalese case of thromboangeitis obliterans or Buerger's disease. Dakar Med. 2006;51:53–6.
[13] Reyes-Gibby CC, Ba Duc N, Phi Yen N, Hoai Nga N, Van Tran T, Guo H, et al. Status of cancer pain in Hanoi, Vietnam: A hospital-wide survey in a tertiary cancer treatment center. J Pain Symptom Manage. 2006;31:431–9.
[14] Shaw E, Kline R, Gillin M, Souhami L, Hirschfeld A, Dinapoli R, et al. Radiation Therapy Oncology Group: radiosurgery quality assurance guidelines. Int J Radiat Oncol Biol Phys. 1993;27:1231–9.
[15] Baltz GC, Chi PM, Wong PF, Wang C, Craft DF, Kry SF, et al. Development and validation of a 3D-printed bolus cap for total scalp irradiation. J Appl Clin Med Phys. 2019;20:89–96.
[16] LeCompte MC, Chung SA, McKee MM, Marshall TG, Frizzell B, Parker M, et al. Simple and Rapid Creation of Customized 3-dimensional Printed Bolus Using iPhone X True Depth Camera. Pract. Radiat Oncol. 2019.
[17] Michiels S, Barragan AM, Souris K, Poels K, Crijns W, Lee JA, et al. Patient-specific bolus for range shifter air gap reduction in intensity-modulated proton therapy of head-and-neck cancer studied with Monte Carlo based plan optimization. Radiother Oncol. 2018;128:161–6.
[18] Low DA, Starkschall G, Sherman NE, Bujnowski SW, Ewton JR, Hogstrom KR. Computer-aided design and fabrication of an electron bolus for treatment of the paraspinal muscles. Int J Radiat Oncol Biol Phys. 1995;33:1127–38.
[19] Hall EJ, Giaccia AJ. Radiobiology for the Radiologist. 7th ed. Philadelphia, PA: Wolters Kluwer Health/Lippincott Williams & Wilkins; 2012.